# Ultrasensitive Doppler based neuronavigation system for preclinical brain imaging applications

Emmanuel Cohen[1,2], Thomas Deffieux[1], Elodie Tiran[1], Charlie Demene[1], Laurent Cohen[2], Mickael Tanter[1]

[1]Institut Langevin, ESPCI ParisTech, PSL Research University, CNRS, UMR 7587, INSERM U979, 75005 Paris, France
[2]University Paris Dauphine, PSL Research University, CNRS, UMR 7534, CEREMADE, 75016 Paris, France

***Abstract*—Ultrasensitive Doppler is a recent medical imaging technique enabling high sensitive acquisition of blood flows which can detect small vascular features without contrast agents. Applied to cerebral imaging of rodents, this method produces very fine vascular maps of the brain at high spatial resolution and leads to functional imaging of brain neuronal activity. These vascular networks contain crucial information about organs structure, and could be used as landmarks to 3D navigate the brain and register external atlas to the data. This study investigates a first step using a 2D correlation-based method to locate in real time young rat, rat, or mouse brain vascular prints in a 3D functional brain atlas.**

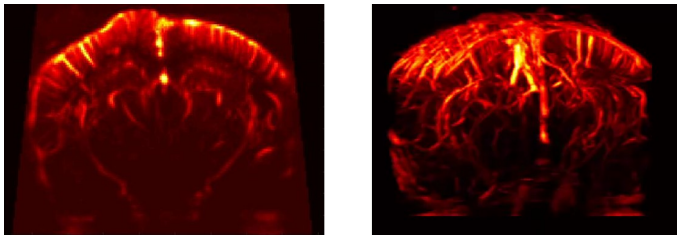

Fig. 1. Left: ultrasensitive Doppler 2D scan of a rat brain coronal section. Right: 3D tomographic reconstruction of a rat brain.

## I. Introduction

### A. Background

Medical ultrasound imaging has become a major clinical technique taking advantage of its portability, its real time working and its low-cost. It allows to achieve an anatomical imaging of high quality which is usually associated to a Doppler examination for blood flows observation and quantification. Nowadays, ultrafast ultrasound imaging enables the observation of very fast variations in the human body like mechanical waves propagation [1] or fast blood flows [2]. In fact, instead of using line-per-line focusing of ultrasonic beams like in standard ultrasound imaging, ultrafast imaging uses ultrasonic plane-wave transmissions associated to the power of graphical processing unit based platforms, in order to accelerate typical frame rates to more than 1000 frames per second [3]. Among these new ultrasensitive techniques is the ultrasensitive Doppler which allows high sensitive acquisition of small vascular features without contrast agent.

Thus, ultrasensitive Doppler imaging produces very fine 3D vascular maps of the rodent brain with high spatial resolution. The acquisition is realized in vivo thanks to a simple mechanical system described in [4]. A mechanical scanning process acquires successive 2D sections along the rodent brain surface for several different orientations. Using a tomographic approach, a post-processing treatment of the data reconstructs a real 3D volume of the cerebral vascular network.

### B. Motivation and objective

The cerebral vascular network contains crucial information about organ structures and could be used as landmark to help clinicians to locate in real time the position of the observed image plane in the patient brain. Such a system would be of great use on human given that now, after injection of microbubbles, ultrafast ultrasonic techniques lead to non-invasive vascular brain imaging on rodents even in the presence of the skull, as shown in [5].

Given any ultrasensitive Doppler in vivo 2D acquisition of the rodent brain, our goal is to give an anatomic description of the observed brain structures in real time, using the vascular print as landmark. This should be feasible for two main reasons. First, some of the observed blood flows closely match the shape of brain structures that can be recognized. Thus, image processing techniques should allow the registration of an external atlas to the data. Secondly, if we assume that the rodent brain vascular network has invariant characteristic vessels, those vessels whose position in the brain is known would be used to localize the position of the acquired image plane. In this study, we investigate the first approach and propose a correlation-based method in order to register an atlas of brain structures to the acquired vascular data.

## II. Materials

In vivo experiments were performed on anesthetized young rats, rats, and mice using ultrasensitive Doppler. Ultrafast ultrasonic imaging enables fast acquisition of brain sections at 100$\mu$m x 100$\mu$m resolution in the image plane. A 15MHz motorized probe acquires 400$\mu$m-thick brain sections with 200$\mu$m spacing. A typical 3D scan of the total width of the rodent brain along one specific direction contains around 35, 65, and 70 sections respectively for young rat, rat, and mouse. A tomographic reconstruction can be achieved from several scan acquisitions along 18 different orientations, to obtain 3D high spatial resolution volume of 100$\mu$m x 100$\mu$m x 100$\mu$m pixel size. A complete description of the experimental set up

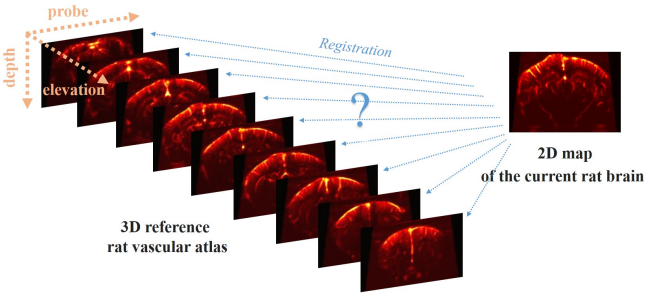


Fig. 2. Description of the monomodal registration strategy adopted: a 2D map of the current rat brain is registered to a 3D reference rat vascular atlas of the same ultrasensitive Doppler image modality.

can be found in [4]. Throughout the rest of the document, we will call probe and depth the two axis of the image plane and elevation the axis of the motor displacement (see figure 2).

## III. Method

### A. Strategy

For simplicity purposes, only acquisitions of coronal sections of the brain were considered. This assumption may not be so strong since a typical Doppler examination in the three directional planes (coronal, sagittal, axial) gives a first satisfying overview of the brain to the clinician. The extension of the method in the sagittal and axial planes may also be almost straightforward.

Direct registration of an atlas of structures to the Doppler acquisition might be difficult to realize. It is in fact a multimodal registration problem that would imply complex 2D curve detection techniques. Of course, one can easily automatically detect some simple geometric features on Doppler images, such as the surface of the skull, an axis of symmetry, or even some circular or elliptic identifiable shapes. However, ultrafast ultrasonic images contain much more discriminating features, and such a basic feature representation is not enough to accurately estimate the position of the image acquisition in the brain atlas.

Therefore, we adopt here a monomodal strategy illustrated by figure 2: an attempt to solve the problem would be to first register the acquired Doppler image to a 3D reference Doppler scan of the whole rodent brain; then, if the reference dataset is previously manually registered to an external atlas, one can superimpose the corresponding atlas section onto the initial observed acquisition.

### B. Registration procedure

We used an intensity-based registration approach. The idea is to correlate the acquired image with every scan image of the reference and consider the maximum of correlation as the correct matching plane. Since the observed brain anatomy is a priori different from the reference one and the parameters of the motorized acquisition may differ from one another, one needs to correlate a geometric transformation of the acquired image to make the correlation successful. We used a linear model consisting in two translations in the image plane (along the probe and depth directions) and one rotation around the elevation axis. Finally, once we detect the best reference matching plane associated to the best matching geometric transformation, we can superimpose the matching atlas section onto the acquired image.

Here is the detailed registration procedure:

- Input data: a test image $\mathbf{I}$ of size $m \times n$, a reference scan $\mathbf{V}$ of size $m \times n \times k$.
- Let $\mathbf{t} = (t_x, t_y, \theta)$ be a linear transformation; apply reverse image warping to $\mathbf{I}$ to get the transformed image $\mathbf{I_t}$.
- Correlate $\mathbf{I_t}$ with all the $k$ stacked scan images of $\mathbf{V}$, and store the largest correlation coefficient $c_\mathbf{t}$ with the index $d_\mathbf{t} \in [\![1, k]\!]$ of the corresponding scan image.
- Repeat the two previous steps for all transformations $\mathbf{t} \in [\![-T_x, T_x]\!] \times [\![-T_y, T_y]\!] \times [\![-\Theta, \Theta]\!]$, and get a correlation matrix $\mathbf{C}$ and a matrix of indexes $\mathbf{D}$ of sizes $(2T_x+1) \times (2T_y+1) \times (2\Theta+1)$, respectively containing all $c_\mathbf{t}$ and $d_\mathbf{t}$.
- Store $d_{\mathbf{t}_{\max}}$ the $\mathbf{D}$-coefficient corresponding to the largest coefficient of $\mathbf{C}$.

The index $d_{\mathbf{t}_{\max}}$ is the index of the best reference matching plane, and $\mathbf{t}_{\max}$ the corresponding geometric transformation. The correlation operator used is as follows:

$$c_\mathbf{t} = \max_k \frac{\sum_{i,j} \mathbf{I_t}(i,j)\mathbf{V}(i,j,k)}{\sqrt{\sum_{i,j} \mathbf{I_t}^2(i,j)}\sqrt{\sum_{i,j} \mathbf{V}^2(i,j,k)}}. \quad (1)$$

Instead of fixing the transformation $\mathbf{t}$ and computing the correlation with all the $k$ images of $\mathbf{V}$, an equivalent second procedure is to fix the correlated reference image $\mathbf{V}_d$ of index $d \in [\![1, k]\!]$, compute the correlation between $\mathbf{V}_d$ and all the possible transformed images $\mathbf{I_t}$, then store the transformation $\mathbf{t}_d$ corresponding to the maximum of correlation $c_d$. Finally, the index $d_{\max}$ corresponding to the largest value among the $k$ coefficients $\{c_d\}_{d=1,..,k}$ is equal to $d_{\mathbf{t}_{\max}}$ of the first procedure, and $\mathbf{t}_{d_{\max}} = \mathbf{t}_{\max}$. This second procedure is clearly more time-consuming because we recompute $k$ times each $\mathbf{I_t}$ whereas in the first procedure there is only one computation. Nevertheless, it will be useful in the context of multiple acquisitions (see IV-A).

## IV. Results

### A. Registration from multiple acquisitions

It may occur that the registration procedure fails for different reasons such as noisy or corrupted data. Therefore, it is in practice more robust to register several different Doppler acquisitions of the same observed rodent brain, and then try to estimate a geometric transformation of the whole test brain by linear regression.

Figure 3 illustrates the second registration procedure (described in III-B) applied to all sections of a test scan dataset of a young rat brain. The reference dataset is from another young rat brain. Here, only two translation degrees of freedom in the image plane are used to compute $\mathbf{I_t}$. On the (a) correlation

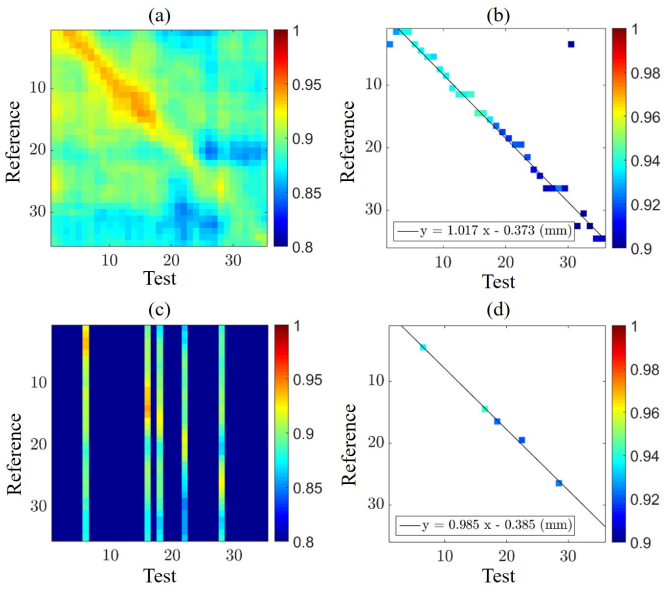


Fig. 3. Registration from multiple acquisitions on a young rat brain: (a) correlation matrix whose each column $d$ contains the correlation coefficients of the $d$-th test section with all the reference ones; (b) maximums of correlation of the matrix in (a); (c)-(d) the same matrices as (a)-(b) but for only 5 test sections.

matrix, each column of abscissa $d$ shows the 35 correlation coefficients $c_d$ of the test section of index $d$ with the 35 reference sections. On (b), we keep only the largest coefficients of each column of the previous matrix. One can observe that the largest coefficients are mostly concentrated on a line near the diagonal, but some apparent outlier points reveal that the registration system can misidentify the good matching reference section. Actually, the quality of these young rat data makes the number of outliers very small. But in general it is not the case, and one would prefer to acquire more than one test Doppler section, in order to estimate by linear regression the global shift in the elevation direction between test and reference brains. This is what is shown by the graphs (c) and (d) where 5 random test sections are registered; the shift in elevation is then evaluated by the intercept of the regression line to 385 $\mu$m (a difference of about 2 sections between both datasets). This last value is very closed to 373 $\mu$m which is the shift found by the linear regression with all test sections on figure (b). It means that only few test sections are required to register a Doppler acquisition.

From these last observations, let notice the practical interest to use the second registration procedure. In fact, it enables a 2D matrix visualization (figure 3(a)) of the correspondence between test and reference sections. In addition, the largest correlation coefficients can be identified by taking either the maximum value of each matrix column (figure 3(b)) or the maximum value of each matrix line. The identification from matrix lines gives an overview of the case where the role of test and reference datasets are inverted.

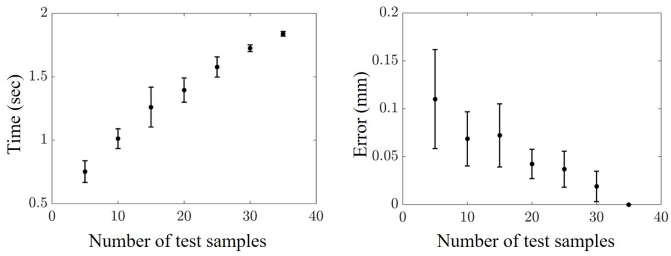


Fig. 4. Left: the computing time (in seconds) of the second registration procedure as a function of the number of test samples; right: the corresponding errors (in millimeters) on the estimated registration parameter in elevation.

### B. Implementation

In order to make the proposed system work in real time, we developed a C++ multithreading implementation using 7 cores. The registration from multiple acquisitions is thus divided into 7 parallel procedures of equal computing time. As a consequence, the correlation matrix figure 3(a) is computed in 1.9 seconds. If we reduce the number of registered test images to 5 (figure 3(c)), the computing time decreases to 0.75 seconds. However, it affects the accuracy of the linear regression with an error of 100$\mu$m on the estimation of the shit in elevation between test and reference datasets. Figure 4 shows on the left the computing time and on the right the error on the shift estimation as functions of the number of registered test samples. As expected, the computing time and the error are respectively increasing and decreasing functions of the number of test sections.

Besides, we also developed a CUDA implementation to improve the computing time performance for rats and mice whose brain is bigger than young rat one. With 3 degrees of freedom for the geometric transformation $\mathbf{t}$, the system can register a rat brain acquisition with 65 reference sections in 1.2 second.

### C. Pre-processing

The correlation calculation can be skewed by noisy pixels. Therefore, we systematically apply a threshold filter to the data before launching the registration procedure. It allows to correlate only relevant pixels which are those with greatest intensity, and reduces by the way the computing time.

When the contrast is low, results can be improved by increasing the image contrast using for instance an algorithm of histogram equalization like CLAHE [6].

### D. Neuronavigation results

We tested the registration process on different rodent brains. The different simulations give more or less good results depending on the quality and the experimental conditions of the acquisition. On young rats and mice, we obtain very few outliers estimations of $d_{\mathbf{t}_{\max}}$. Figure 5 shows the results of the first registration procedure applied to mice scans. On the bottom-right graph, the matching indexes $d_{\mathbf{t}_{\max}}$ between test and reference datasets are plotted forming a quasi-straight line with very few outliers. The three other graphs show the

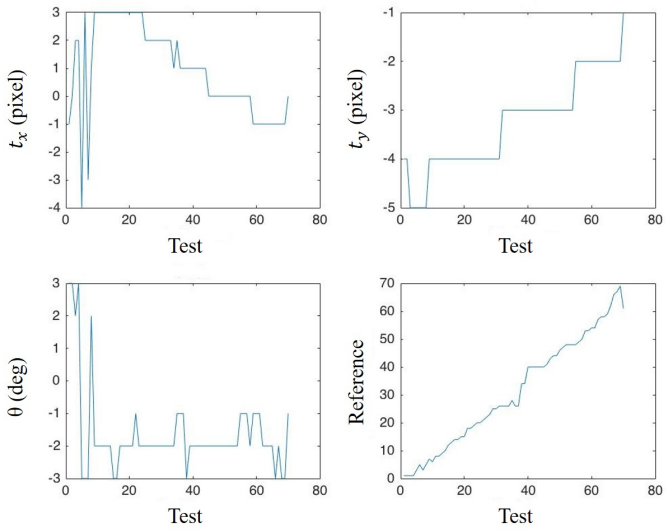


Fig. 5. Results of the first registration procedure on mice Doppler scans. On the first 3 graphs is shown the progression of the estimated registration parameters $\mathbf{t}_{\max} = (t_x, t_y, \theta)_{\max}$ (in pixels and degrees). The bottom-right graph shows the matching reference section indexes as a function of test sections indexes.

estimated transformation parameters $\mathbf{t}_{\max} = (t_x, t_y, \theta)_{\max}$, from which test and reference datasets can be registered along the two other (probe and depth) directions. We observe that both $t_x$ and $t_y$ follow linear progressions and $\theta$ seems to be constant along the elevation axis. For young rats, we described in IV-A the good performance of the second registration procedure, illustrated by figure 3.

In order to improve the results, one should improve the robustness of the image matching algorithm to the quality of the data. A first attempt consists in choosing a reference dataset of high quality and high resolution. Therefore, we tested the second registration procedure considering a 3D tomographic reconstruction of the rat brain as the reference dataset. The latter volume is of high quality and with a two times higher spatial resolution in the elevation direction than a 3D scan (see II). Using a high resolution reference dataset is of great interest since any test acquisition of lower resolution and of any brain section could be thus registered by bringing the reference resolution to the test one. Figure 6 shows the fairly successful result of the registration of a 3D test scan dataset to the high resolution one. The left image shows a manual superimposition of the Paxinos atlas [7] onto a high resolution reference section. After a few seconds of processing the registration algorithm, one can navigate the test scan dataset, as illustrated by the right image where we show the automatic superimposition of the Paxinos atlas on a test scan section.

## V. Conclusion

In this study, we proposed a real time correlation based system to 3D navigate the rodent brain from ultrasensitive Doppler. The system uses a typical number of 5 different 2D acquisitions of the brain to compute in a few seconds its 3D registration with a well suited reference dataset. The monomodal registration strategy adopted involves sophisticated techniques from image and pattern matching. In a future work, this first correlation based solution could be improved by using a more robust algorithm based for instance on sparse representation of images.

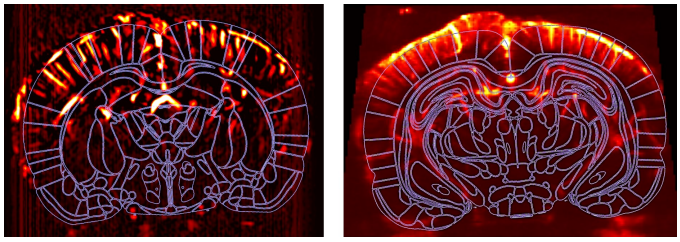

Fig. 6. Left: manual superimposition of the Paxinos atlas on a section of a rat brain 3D tomographic reconstruction. Right: automatic superimposition of the Paxinos atlas on a registered rat brain scan acquisition.

## References

[1] J.-L. Gennisson, T. Deffieux, M. Fink, and M. Tanter, "Ultrasound elastography: principles and techniques," *Diagnostic and interventional imaging*, vol. 94, no. 5, pp. 487–495, 2013.

[2] J. Bercoff, G. Montaldo, T. Loupas, D. Savery, F. Meziere, M. Fink, and M. Tanter, "Ultrafast compound doppler imaging: providing full blood flow characterization," *IEEE transactions on ultrasonics, ferroelectrics, and frequency control*, vol. 58, no. 1, pp. 134–147, 2011.

[3] M. Tanter and M. Fink, "Ultrafast imaging in biomedical ultrasound," *IEEE transactions on ultrasonics, ferroelectrics, and frequency control*, vol. 61, no. 1, pp. 102–119, 2014.

[4] C. Demené, E. Tiran, L.-A. Sieu, A. Bergel, J. L. Gennisson, M. Pernot, T. Deffieux, I. Cohen, and M. Tanter, "4d microvascular imaging based on ultrafast doppler tomography," *NeuroImage*, vol. 127, pp. 472–483, 2016.

[5] C. Errico, J. Pierre, S. Pezet, Y. Desailly, Z. Lenkei, O. Couture, and M. Tanter, "Ultrafast ultrasound localization microscopy for deep super-resolution vascular imaging," *Nature*, vol. 527, no. 7579, pp. 499–502, 2015.

[6] K. Zuiderveld, "Graphics gems iv," P. S. Heckbert, Ed. San Diego, CA, USA: Academic Press Professional, Inc., 1994, ch. Contrast Limited Adaptive Histogram Equalization, pp. 474–485. [Online]. Available: http://dl.acm.org/citation.cfm?id=180895.180940

[7] G. Paxinos and C. Watson, "The rat brain atlas in stereotaxic coordinates," *San Diego: Academic*, 1998.